

Fitts' Law for speed-accuracy trade-off is a diversity sweet spot in sensorimotor control

Yorie Nakahira^{1,4}, Quanying Liu^{1,4}, Terrence J. Sejnowski^{2,3*}, John C. Doyle^{1*}

¹Division of Engineering and Applied Science, California Institute of Technology,
Pasadena, CA 91125, USA

²The Salk Institute for Biological Studies, La Jolla, CA, USA

³Division of Biological Sciences, University of California, San Diego, La Jolla, CA, USA

⁴These authors contributed equally

*To whom correspondence should be addressed; E-mail: doyle@caltech.edu, terry@salk.edu.

Human sensorimotor control exhibits remarkable speed and accuracy, as celebrated in Fitts' law for reaching. Much less studied is how this is possible despite being implemented by neurons and muscle components with severe speed-accuracy tradeoffs (SATs). Here we develop a theory that connects the SATs at the system and hardware levels, and use it to explain Fitts' law for reaching and related laws. These results show that *diversity* between hardware components can be exploited to achieve *both* fast *and* accurate control performance using slow or inaccurate hardware. Such “diversity sweet spots” (DSSs) are ubiquitous in biology and technology, and explain why large heterogeneities exist in biological and technical components and how both engineers and natural selection routinely evolve fast and accurate systems from imperfect hardware.

Human sensorimotor control is remarkably fast and accurate despite being implemented using slow or inaccurate components (1–6). For example, Fitts’ Law predicts that, in many forms of reaching (e.g. eye gaze, hand, mouse), the time required for reaching quickly to a target of width W at distance D scales as $\log_2(2D/W)$ (7, 8). The logarithmic relation between the reaching time and target width allows faster speed to be achieved with a small decrement in accuracy. On the other hand, the speed-accuracy tradeoffs (SATs) of the hardware implementing control can be much more severe. Improving either speed or accuracy in nerve signaling or muscle actuation requires profligate biological resources (6); as a consequence, only a few types of nerves and muscles are built to be both fast and accurate (Fig. 1). Such apparent discrepancy between the speed-accuracy tradeoffs in sensorimotor control and neurophysiology poses the question: how does nature deconstrain neurophysiological hardware constraints in sensorimotor control?

In this paper, we develop a networked control system model to relate the SATs in sensorimotor control and neurophysiology. The model characterizes how hardware SATs in nerves and muscles impose fundamental limits in sensorimotor control and recovers Fitts’ Law as a special case. The results show that appropriate speed-accuracy diversity at the level of neurons and muscles allow nervous systems to improve the speed and accuracy in control performance despite using slow or inaccurate hardware, which we call “Diversity Sweet Spots.”

We consider a feedback loop in Fig. 2A. Here, the error between the actual position and the desired position $x(t+1)$ is computed from the previous error $x(t)$, the sensed uncertainty $w(t)$, and the control action $u(t)$ as follows:

$$x(t+1) = x(t) + w(t) + u(t). \quad (1)$$

The control action, characterized by \mathcal{K} , is generated from the observed errors, sensed uncer-

tainty, and past control actions, *i.e.*

$$u(t + T) = \mathcal{K}(x(0 : t), w(0 : t - 1), u(0 : t + T - 1)). \quad (2)$$

using sensing components such as eyes and muscle sensors; communication components such as nerves; computing components such as the cortex in the central nervous system; and actuation components such as eye and arm muscles. The total delay from the disturbance to the control action is given by $T := T_s + T_i$, where T_s captures the latency in nerve signaling, and T_i captures other internal delays in the feedback loop. We constrain that the feedback loop can only transmit R bits of information per unit time (denote as signaling rate) (9). Table S1 in the Supplementary Material summarizes the above parameters.

The communication components, axons in sensory nerves or motor neurons, carry sensory information from the periphery into the brain and activate muscles in the final common pathway. There exist heterogeneity in the size and number of axons within a nerve bundle and between different types of sensory nerves, with calibers in mammals ranging over two orders of magnitude from tenths of microns to tens of microns (10–13). This size and number heterogeneity lead to extreme differences in neural signaling speed and accuracy as the speed and rate of information flow in an axon depend on its diameter and myelination. To quantify the bundle of axons in certain nerves, we model axon bundles as a communication channel with signaling delay T_s and signaling rate R . Building upon (6) and references therein, we show in the Supplementary Materials that, under some assumptions, the nerve signaling SAT can be modeled by

$$R = \lambda T_s. \quad (3)$$

where λ is proportional to the spatial and metabolic cost to build and maintain the nerves. The nerve signaling SATs differ from species to species and increase in animal size (13, 14). Eq. 3 can be refined or modified given specific types of nerves or encoding mechanisms, but the rest

of our framework does not require the component SATs to have any specific form. So for the rest of this paper, we use Eq. 3 to demonstrate how the SATs at the component level impact those at the system level.

The actuation components, muscle, also have tradeoffs in terms of the reaction speed, accuracy in strength level, maximum strength, and ease of fatigue. Moreover, most muscles carry diverse muscle fibers, *e.g.*, striated muscles typically have both large fast twitch fibers and many more smaller slow twitch muscles (Fig. 1B). In particular, its SATs can be modeled using a simplified muscle model that includes m motor units, indexed by $i \in \{1, 2, \dots, m\}$, each associated with a reaction speed and a fixed strength. We use F_i to denote its strength and assume without loss of generality that $F_1 \leq F_2 \leq \dots \leq F_m$. According to Henneman's size principle (15), motor units in the spinal cord are recruited in ascending order of F_i , so a muscle (at non-transient time) can only generate $m + 1$ discrete strength levels: $\sum_{i=1}^n F_i$, where n can take any integer from 0 to m . Given a fixed length, the maximum strength of a muscle $\ell = \sum_{i=1}^m F_i$ is known to be proportional to its cross-sectional area (16). This implies that, given a fixed space to build a muscle, its maximum strength does not depend on the specific composition of motor units. Constrained on the maximum strength, a muscle can be built from many motor units with small strengths or a few motor units with large strengths. In the former case, the muscle has better resolution but slower reaction speed, while in the latter case, the muscle has faster reaction speed but coarser resolution (see Fig. S2 in the Supplementary Material). This SAT can be quantified using the following formula:

$$\dot{a}_i(t) = \alpha f_i^p(t)(1 - a_i(t)) - \beta a_i(t) \quad a_i^q(t) = c_i(t) \quad (4)$$

where $\alpha = 1, \beta = 1, p = 1, q = 3$ are fixed constants (17). If a motor unit is recruited at time $t = 0$, then its strength $c_i(t)$ rises according to Eq. 4 with $f_i(t) = 1(t)/((1/F_i)^{1/q} - 1)$, where $1(t)$ is a unit step function. Similarly, when a recruited motor unit is released at time $t = \tau$, its

contraction rate falls according to Eq. 4 with $f_i(t) = 1(-t + \tau)/((1/F_i)^{1/q} - 1)$. From Eq. 4, the reaction speed of a muscle is an increasing function of F_i (18), so better resolution (having small F_i) can only be achieved with decreased reaction speed.

Next, we use the basic model (Eq. 1 and Eq. 2) to study how the nerve SATs impact the system SATs in reaching. In a reaching task, the subjects' goal is to move their hand or cursor to a target as rapidly and accurately as possible. This setting can be recovered by setting $w(t) = d\delta(t)$ in Eq. 1, where $d \in [-D, D]$ is the distance between the initial position and the target position, and $\delta(t)$ is the Kronecker delta function (19). There exist tradeoffs between the reaching speed and accuracy, where the speed of reaching is quantified by the reaching time T_r (*i.e.* time taken to reach the target area), and the accuracy is quantified by normalized target width W/D . The relation between T_r and D/W satisfies

$$\sup_{|d| \leq D} T_r \geq T + \frac{1}{R} \log_2(2D/W). \quad (5)$$

This formula recovers Fitts' law (8, 20), which states that the reaching time follows $T_r = p + q \log_2(2D/W)$, where $F := \log_2(2D/W)$ is called the Fitts' index of difficulty, and p and q are fixed constants. The proof of Eq. 5 can be found in the Supplementary Material, but its intuition can be obtained as follows: identifying a target of width W in range $[-D, D]$ requires F bits of information, and transmitting F bits of information requires F/R time steps with additional T time steps of (transmission) delay in the feedback loop.

Eq. 5 decomposes into two terms: the term T that is only a function of the delay, and the term $\frac{1}{R} \log_2(2D/W)$ that is only a function of the data rate. Therefore, we can consider the first term as the cost in reaching time due to having delay in the feedback loop (denote as the delay cost), and the second term as the cost due to having limited data rate in the feedback loop (denote as the rate cost). By combining the component-level SATs in Eq. 3 and the system-level SATs in Eq. 5, we can predict how the SATs in neural signaling impact sensorimotor control

in Fig. 3A. Eq. 5 suggests that the signaling delay T_s affects the reaching time T_r in a linear manner, whereas the signaling rate R affects T_r in an inversely proportional manner.

We tested these theoretical predictions with reaching experiments (Fig. 2B,C). The subjects were asked to control a steering wheel with added delays, quantization, and both (see the Supplementary Material for details), and their reaching times for each case are shown in Fig. 3B. Fig. 3 suggest that axon compositions that minimize either the signaling delay or the rate alone suffer from large delay or rate costs, rendering the system suboptimal. Conversely, the minimum reaching time is achieved when both the signaling delay and rate are chosen to be moderate levels, leading to a minimum delay plus rate costs. In particular, subject to the nerve SAT Eq. 3, the minimum reaching time is achieved at $T = \sqrt{F/\lambda}$, $R = \sqrt{\lambda F}$. The optimal T and R is increasing/decreasing in F . This is because as the index of difficulty F increases, the reaching task requires more accuracy, and the data rate limit gains greater impact on the reaching time. Thus, for a reaching task with large F , fast reaching times are achieved with increased data rate R at the expense of increased delay T .

The dependencies of optimal nerve signaling speed and accuracy (T, R) on F suggests that diversity in signaling speed and accuracy allows better reaching performance with a broad range of difficulties. Indeed, there exists heterogeneity in the size and number of axons within a nerve bundle and between different types of sensory nerves, with calibers in mammals ranging over two orders of magnitude from tenths of microns to tens of microns (11–13). As the speed and rate of information flow in an axon depend on its diameter and myelination (21, 22), this size and number heterogeneity lead to extreme differences in neural signaling speed and accuracy.

Eq. 5 assumes that the SATs in nerve signaling are the bottleneck in the reaching task. Although this assumption is valid for certain eye movements or small-distance reaching, in many other types of reaching tasks, muscle actuation SATs is the major limiting factors in the reaching SATs. To understand how the muscle SATs impact the reaching SATs, we model the

sensorimotor system by Eq. 1 and Eq. 2 with limited muscle actuation SATs, which is obtained from Eq. 4.

We compare the reaching SATs when the muscle (actuation component) contains uniform versus diverse motor units in Fig. 4A. Having diversity within muscles largely improves the reaching SATs because having large motor units and small ones help have better speed and accuracy in sensorimotor control than having uniform motor units. Specifically, when muscles are built from diverse motor units, large motor units allow for faster activation at the beginning of a reaching, while small motor units can be used to fine-tune the force toward the end of reaching.

We confirmed the benefit of diversity using reaching experiments (Figs. 2B,C,S5). In the experiments, subjects were asked to move to a target of fixed width as fast as possible under two settings: using uniform speed or diverse speeds. Fig. 4B compares their reaching SATs when only one level of speed was allowed versus when two levels of speed were allowed versus. The performance under diverse speed largely outperforms that under uniform speed. Moreover, a uniform speed gave rise to a linear SAT which is not consistent with the logarithmic form of Fitts' law, while the flexibility to use diverse speeds yielded a DSS like Fitts' law, in which fast reaching can be performed accurately. Although the logarithmic form of Fitts' law has been confirmed in many experiments and explained using various models (see (8, 20, 23–25) and references therein), our results reveal that Fitts' law arises from DSSs, in which the hardware diversity is key for achieving fast and accurate performance using slow or inaccurate hardware. This relation of DSSs and logarithmic laws potentially provide new insights into other logarithmic laws observed (26).

DSSs may also help us understand how engineered systems can achieve fast and accurate performance with slow or inaccurate components. For example in a transportation system, no single mover (*e.g.* walking, driving, flying) can rapidly take you from one point on the earth to

another. But a combination of an airplane that rapidly takes you from one city to another, and ground transportation, which can take you more slowly from one part of a city to another, and walking, which can take you even more slowly from one point to another, can together achieve fast and accurate transport (see the Supplementary Material).

Although this paper focuses on the benefit of hardware diversity and its connection to Fitts law, DSSs can also be observed in the layered architectures used in different types of sensorimotor control, such as the control of eye movements (4, 5), and decision making in general (27–29). Take an example of our visual system, involving diverse control layers. The vestibulo-ocular reflex is a layer that performs fast but inaccurate negative feedback control to stabilize images on the retina against rapid head movements. This layer works in concert with another layer that performs smooth pursuit, a slow but accurate cortical system for tracking slowly moving visual objects. These two layers jointly create a virtual eye controller that is both fast and accurate. More detail about DSSs in layered control architectures, like the visual system, is presented in our companion paper (30). More generally, DSSs may reveal a more general design principle for distributed control in brains and inspire the design of large-scale technological systems.

References and Notes

1. E. Todorov, M. I. Jordan, *Nature neuroscience* **5**, 1226 (2002).
2. A. J. Nagengast, D. A. Braun, D. M. Wolpert, *Journal of neurophysiology* **105**, 2668 (2011).
3. D. W. Franklin, D. M. Wolpert, *Neuron* **72**, 425 (2011).
4. S. Lac, J. L. Raymond, T. J. Sejnowski, S. G. Lisberger, *Annual review of neuroscience* **18**, 409 (1995).
5. S. G. Lisberger, *Neuron* **66**, 477 (2010).
6. P. Sterling, S. Laughlin, *Principles of neural design* (MIT Press, 2015).
7. P. M. Fitts, J. R. Peterson, *Journal of experimental psychology* **67**, 103 (1964).
8. Fitts's law (wikipedia).
9. A summary of the parameters used is given in **Table S1**.
10. J. A. Perge, J. E. Niven, E. Mugnaini, V. Balasubramanian, P. Sterling, *Journal of Neuroscience* **32**, 626 (2012).
11. J. Stenum, *Journal of Experimental Biology* **221**, jeb170233 (2018).
12. H. L. More, *et al.*, *Journal of Experimental Biology* **216**, 1003 (2013).
13. H. L. More, *et al.*, *Proceedings of the Royal Society B: Biological Sciences* **277**, 3563 (2010).
14. Bigger animals have more inertia and can tolerate longer delays. they also use more time to compute in part because large animals (elephants, etc.) are more prone to falling.

15. E. Henneman, G. Somjen, D. O. Carpenter, *Journal of neurophysiology* **28**, 560 (1965).
16. G. Goldspink, *Journal of experimental biology* **115**, 375 (1985).
17. V. Brezina, I. V. Orekhova, K. R. Weiss, *Journal of neurophysiology* **83**, 207 (2000).
18. In other words, the time required for a muscle to reach to $c_i(t) = f_i$ from $c_i(0) = 0$ is decreasing in f_i .
19. The Kronecker delta function is defined as follows: $\delta(t) = 1$ if $t = 0$, and $\delta(t) = 0$ otherwise.
20. P. M. Fitts, *Journal of experimental psychology* **47**, 381 (1954).
21. A. Hodgkin, *The Journal of physiology* **125**, 221 (1954).
22. D. Hartline, D. Colman, *Current Biology* **17**, R29 (2007).
23. T. O. Kvåiseth, *Perceptual and Motor Skills* **49**, 291 (1979).
24. I. S. MacKenzie, *Journal of motor behavior* **21**, 323 (1989).
25. H. Hatze, *Bulletin of mathematical biology* **41**, 407 (1979).
26. These laws include the weber-fechner law, a log relation between the physical change in a stimulus and the perceived change in human perception; the ricco law for visual target detection for unresolved targets; the accot-zhai law for steering, a generalization of fitts' law for 2d environments; the spacing effect of ebbinghaus for long-term recall from memory; and the hick-hyman law for the logarithmic increase in the time it takes to make a decision as the number of choices increases.
27. D. Kahneman, P. Egan, *Thinking, fast and slow*, vol. 1 (Farrar, Straus and Giroux New York, 2011).

28. N. R. Franks, A. Dornhaus, J. P. Fitzsimmons, M. Stevens, *Proceedings of the Royal Society of London. Series B: Biological Sciences* **270**, 2457 (2003).
29. L. Chittka, P. Skorupski, N. E. Raine, *Trends in ecology & evolution* **24**, 400 (2009).
30. Y. Nakahira, et. al, Diversity sweet spots in layered architectures and speed-accuracy trade-offs in sensorimotor control. Unpublished.

Acknowledgments

This research was supported by National Science Foundation (NCS-FO 1735004 and 1735003). Q.L. was supported by a Boswell fellowship and a FWO postdoctoral fellowship (12P6719N LV).

Figures

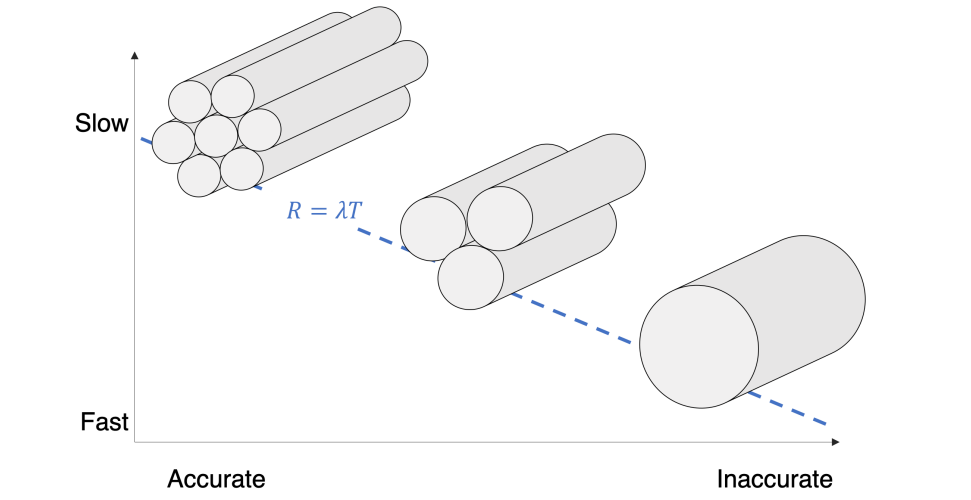
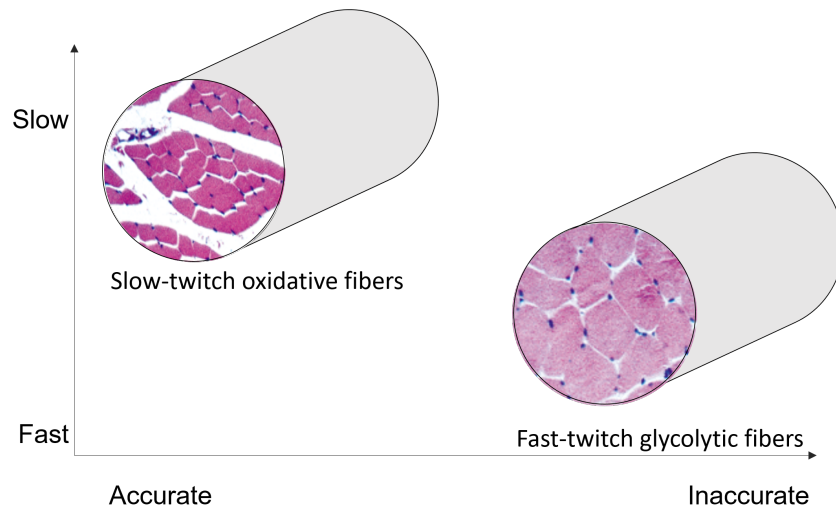
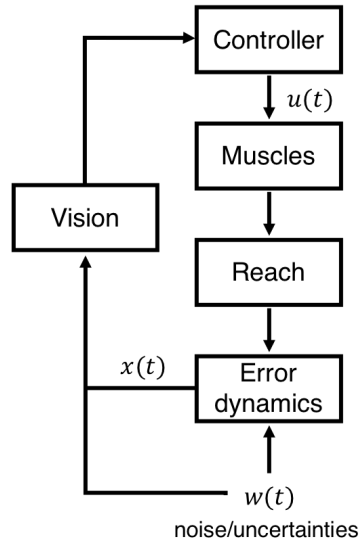
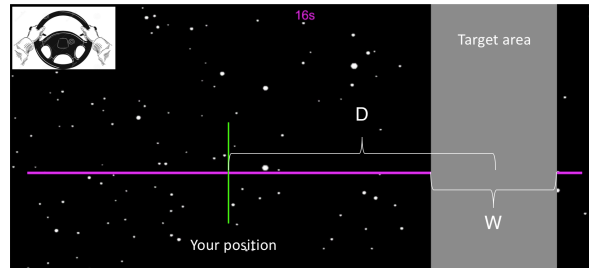
A**B**

Figure 1: Component-level speed-accuracy trade-off (SAT) in nerves and muscles. (A) Cartoon diagram showing how nerve size and number trade-offs result in its signaling SATs. The region above the dashed line represents the achievable speed and accuracy given a fixed total cross-sectional area, which is proportional to λ . (B) Different types of muscle fibers and their resulting actuation SATs. The one with a smaller diameter and darker color (due to larger amounts of myoglobin, numerous mitochondria, and extensive capillary blood supply) are the oxidative fibers, and the other is the glycolytic fibers. Oxidative fibers are slower but more accurate, whereas glycolytic fibers are faster but less accurate.

A



B



C

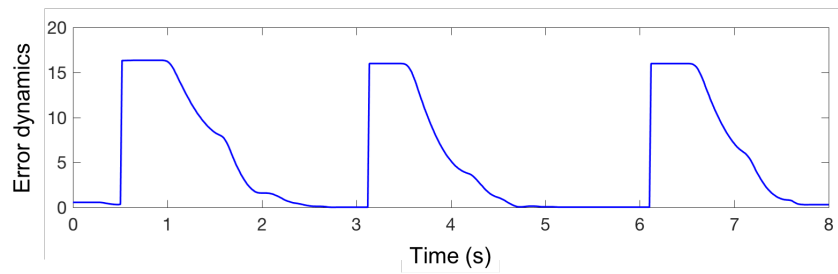


Figure 2: The model and system. (A) Block diagram of the sensorimotor control model that simulates the reaching task. Each box is a component in the model that communicates (vision), computes (controller), or actuates (muscles) with potentially limited speed and accuracy. (B) Video interface for the reaching experiment. The green line indicates the player's position and the gray zone is the target. The subjects' goal is to steer the wheel to reach the target as fast as possible and stay at the target. (C) An error dynamics measured in an experiment. The error $x(t)$ is defined as the difference between the player's position and the center of the target.

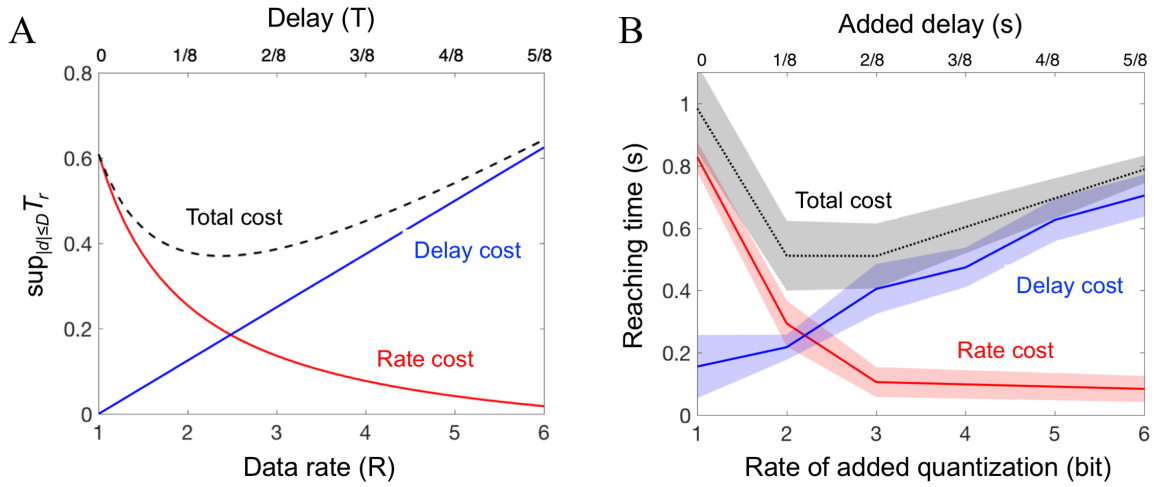


Figure 3: The SATs. (A) Theoretical SATs in the reaching task. The delay cost (blue line), rate cost (red line), and the total cost (dashed black line) in Eq. 5 are shown with varying component SAT $T = (R - 1)/8$. (B) Empirical SAT in the reaching task. Data obtained from 4 subjects who performed the task over a range of time delays and quantization (See Fig. S1 for data from individual subjects). The blue line shows the performance with added actuation delay T ; the red line shows the performance with added quantization of rate R ; and the black line shows the performance with added delay and quantization subject to the SAT $T = (R - 1)/8$. The shaded region around the lines is standard errors.

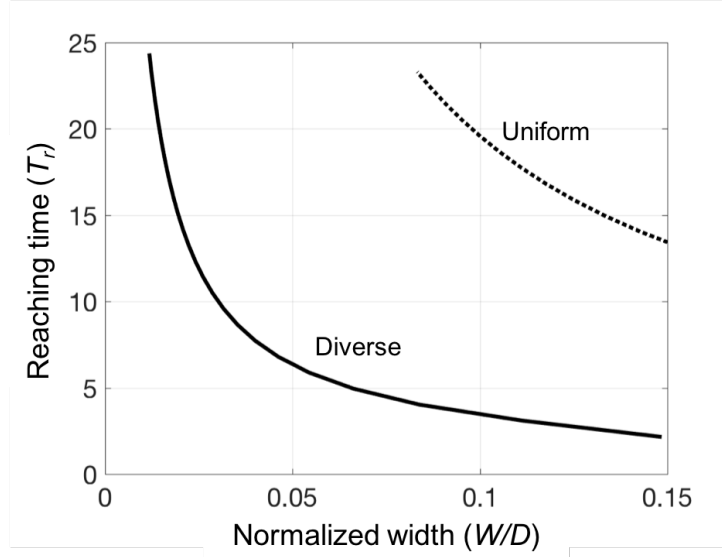
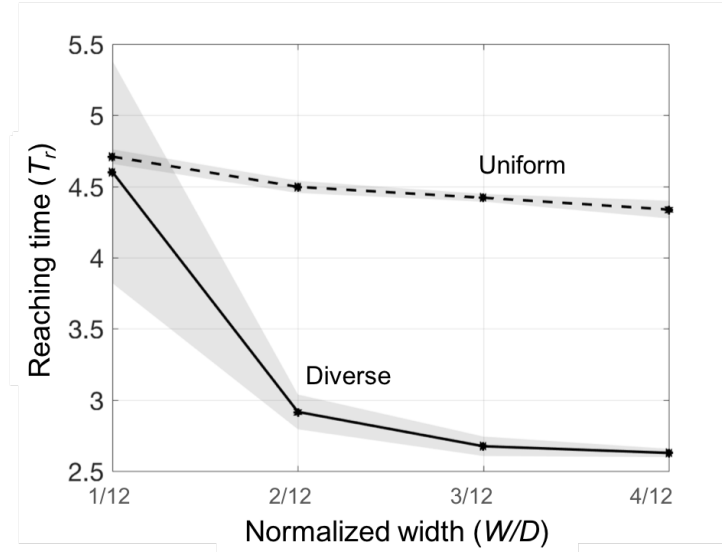
A**B**

Figure 4: Experimental confirmation of predicted diversity advantage in reaching. (A) Theoretical DSSs in the reaching task derived from the SATs of a feedback loop implemented by a muscle composed of uniform (dashed line) or diverse motor units (solid line). The DSSs for two feedback loops with diverse muscles and uniform muscles are shown in FigS4. (B) Benefits from diversity in the reaching task. The plot shows the performance of a subject who performed the reaching task with uniform or diverse speeds, which is designed to mimic the case of uniform or diverse muscles, respectively. See the Supplementary Material for more detail.

Supplementary Material

The nerve signaling SAT

The impact of nerve SATs on reaching SATs

The impact of muscle SATs on reaching SATs

Experimental setting

Diversity sweet spots in transportation

Figs. S1-S5

Table S1

Video S1

References and notes